# Approximate Simulation of Elastic Membranes by Triangulated Spring Meshes

Allen Van Gelder
Computer Science Dept.
University of California, Santa Cruz 95064
E-mail: {avg}@cs.ucsc.edu

March 18, 2004

**Abstract**

Spring meshes have been used to model elastic material in computer graphics, with skin, textiles, and soft tissue being typical applications. A spring mesh is a system of vertices and edges, possibly with highly irregular geometry, in which each edge is a spring, and springs are connected by "pin-joints" ("gimbal-joints" in 3D) at the vertices. This method is computationally attractive, compared to some alternatives. However, given a specified set of elastic material properties, the question of whether a particular spring mesh accurately simulates those properties, has been largely ignored in the literature. Additionally, previous reports on the technique are silent on the subject of assigning stiffness to the various springs. This paper shows that assigning the same stiffness to all springs badly fails to simulate a uniform elastic membrane, for equilibrium calculations. A formula for spring stiffness that provides a more accurate simulation is then derived. In its simplest form, this formula specifies that stiffness varies as triangle area over edge length squared. Its accuracy is demonstrated on test and practical mesh examples. It is also shown that an exact simulation is not possible, in general. Extensions to nonuniform materials and three dimensions are discussed briefly.

## KeyWords

Computer graphics, finite element method, spring mesh, elastic membrane, tissue models.

## 1 Introduction

Discrete models of elastic materials have many applications, particularly in computer graphics. The driving force for this research was the problem of modeling skin so that it would stretch and slide realistically over an underlying body of modeled muscles and bones. Particularly, on animal skin with markings or fur, the markings and hairs should shift realistically in response to underlying limb movements, and so on. For this purpose, skin can be regarded as a uniform, isotropic elastic membrane. However, the results apply equally well to non-uniform, isotropic elastic membranes, as well as to 3D isotropic elastic solids. An isotropic elastic material is one whose *local* deformation in response to force is independent of direction; however this response might vary over space, in which case the material is non-uniform, but still may be isotropic. We have not investigated non-isotropic elasticity.

Our main concerns were that the model arrive at reasonable equilibrium positions within a reasonable amount of computation. In effect we treat the elastic system as highly damped. However, the formulas developed do not depend on this aspect of our application, and are equally applicable to other dynamic environments, where the damping factors would have to be specified, in addition to the stiffness factors.

We assume the membrane is given as a triangulated surface, produced by some independent surface generation process, so we do not have control over the sizes and shapes of the triangles. Elastic properties of the membrane are also specified. Two methods are commonly used to simulate such a membrane:

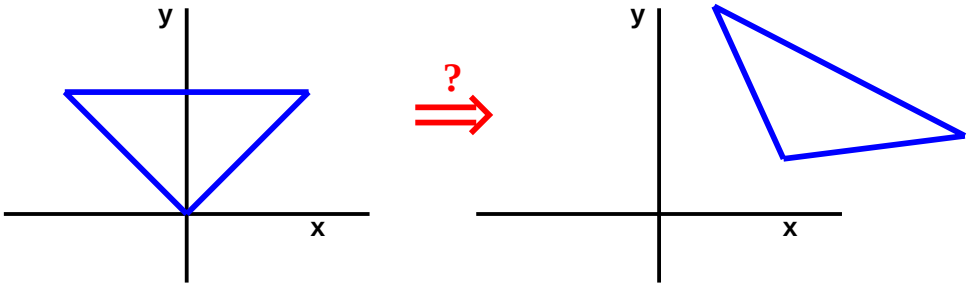


Figure 1: Triangle in rest position at left has arrived at the vertex positions shown at right. The *inverse elasticity problem* is to determine what stresses are now present in the triangle. For the membrane model, this involves decomposing the transformation into a rigid-body motion and a deformation.

1. The traditional *finite element method* models each triangle as an individual elastic membrane, with compatibility conditions to ensure they join correctly after deformation.

2. The *spring mesh* is an alternative seen in computer graphics literature (see Section 1.1). This technique models each *edge* in the triangulated surface as a spring, i.e., an idealized one-dimensional elastic object. Springs are connected as pin joints at the vertices.

The literature seems not to address the question of under what conditions, if any, the second approach produces exactly, or approximately, the same results as the first approach. This paper provides some answers.

Although, as shown in Section 4, triangulated spring meshes cannot exactly simulate an elastic membrane, some practitioners will elect to use spring meshes for two main reasons: conceptual simplicity and computational speed.

To illustrate conceptual simplicity, consider the problem depicted in Figure 1, which might be termed the *inverse elasticity problem*. Suppose we are given that the original triangle at the left is now in the position shown at the right. What internal elastic forces is that triangle producing? This is a completely straightforward problem for the spring-mesh model. For the finite-element membrane model, the solution is not at all obvious.

Issues of computational speed are clearly spelled out in work reviewed below [NG96, VMT97]; the consensus is that spring meshes are at least an order of magnitude faster than more the more accurate finite-element membrane models.

These considerations provide some motivation for the need to have a good approximation method, but are not intended to suggest that spring meshes are generally superior to the higher dimensional elastic model. Which methodology to choose in a given situation depends on many factors.

This paper investigates the connection between the two models, finite-element membranes and spring meshes, with particular attention to finding the spring stiffness coefficients for the second model that allow it to simulate the first model. For dynamical simulations, damping factors are also important, but they are not investigated here.

For a mesh edge $c$, let $|c|$ be its length. The *spring stiffness coefficient*, $k_c$, is defined by the equation $f = k_c \Delta|c|$, where $f$ is the stretching force and $\Delta|c|$ is the change in length in response to $f$. A related parameter is the *one-dimensional Young's modulus*, $E_1 = |c|k_c$. Previous papers have not spelled out a scheme for setting spring stiffness coefficients, leaving the presumption that they are all equal, or in the case of a multi-level model, that they are all equal within each level. Several test cases demonstrate that this choice of making all spring stiffness coefficients equal produces quite noticeable distortions (see Section 6). Another heuristic, to make the one-dimensional Young's modulus constant, also fares badly (also see Section 6).

This paper derives a formula for varying the spring stiffness coefficient of an edge according to the geometry of the triangles incident upon that edge. In its simplest form, this formula specifies that spring stiffness coefficients vary as triangle-area over edge-length squared:

$$k_c = \frac{E_2 \sum_e \text{area}(T_e)}{|c|^2} \tag{1}$$

where the sum is over the (normally two) triangles $T_e$ incident upon edge $c$. The coefficient $E_2$ is technically the two-dimensional Young's modulus (see Section 2) of the membrane to be simulated. In practice it is usually chosen empirically to give the desired amount of stretchiness. The analogous three-dimensional equation for an elastic tetrahedral mesh is

$$k_c = \frac{E \sum_e \mathrm{vol}(T_e)}{|c|^2} \tag{2}$$

where now the sum is over the *tetrahedra* $T_e$ incident upon edge $c$, and the number of such tetrahedra varies.

The remainder of the paper is organized as follows. The remainder of this section reviews related work (Section 1.1). The linear elasticity model is discussed in Section 2, and membranes are reviewed in Section 3. Section 4 shows that an exact simulation between the two models is impossible in general (see Example 4.2). However, in Section 5 we derive a formula for spring stiffness coefficients that enables an irregular spring mesh to simulate uniform elasticity more accurately than previously published methods. Because the formula is local, it extends immediately to the case of non-uniform membranes. A simple extension to three-dimensional meshes (solids rather than membranes) is proposed in Section 5.1. Tests presented in Section 6 show that the approximate formula produces very accurate results for membranes in a variety of cases. Section 7 concludes the paper.

## 1.1 Background

Although a rich literature exists on finite element methods for engineering elasticity, this literature has considered mainly materials that undergo very little deformation within their elastic limits, such as metals, and is more concerned with distribution of forces, rather than the deformation itself [TG51, Whi85, ZT89]. Computer graphics applications are typically more concerned with observable deformations of less rigid materials, such as skin, other soft tissue, fabrics, inflated balls, etc.

Terzopoulos *et al.* introduced the use of elasticity theory for modeling deformable materials into the computer graphics literature [TPBF87], without giving any computation times. The work was extended to inelastic materials [TF88] and to combinations of rigid and deformable materials [TW88]. Terzopoulos and co-authors have more recently applied elastic models to simulation of the face, using a layered model of facial tissue consisting of triangular prism finite elements connected by biphasic springs [TW90, TW91, LTW95]. Later work models fish and animated teapots [TTG95, FVdPT97].

Ng and Grimsdale survey the considerable work on modeling cloth and textiles [NG96]. Volino *et al.* used a finite element membrane model to simulate deformable surfaces such as cloth [VCMT95]. Eischen *et al.* use nonlinear shell theory, and conclude that faster methods are needed [EDC96]. Also, Volino and Magnenat-Thalmann recently developed a mass-spring model to achieve faster performance than their membrane model [VMT97]. Baraff and Witkin report further advances in cloth simulation by better mathematical techniques [BW98].

Miller used a simple elastic spring-mesh model with fixed spring stiffness coefficients to model the motion of snakes and worms [Mil88]. Chen and Zeltzer used a finite element model to simulate a skeletal muscle [CZ92]. Isometric brick elements were used.

Celniker and Gossard [CG91] used finite elements for general free-form modeling. Primitives automatically deformed to minimize energy based on user-supplied values. Curve and surface elements were used.

Koch *et al.* recently described the use of finite element models for simulating facial surgery [KGC+96]. They process photogrammetric and CT scan data of the face to create a finite element model of the facial surface and soft tissue. Stiffness parameters depend on the type of material modeled: bone, skin, muscle, or fat. A globally C1 continuous finite element model with nonlinear shape functions, based on triangular prism elements, is developed.

In the above cited research, elastic materials are represented as spring meshes in several cases. These papers mostly either explicitly state that the stiffness coefficients of these springs are independent of the geometry (but often depend on the material), or they imply it by not giving any method to choose the values. As we shall show experimentally, for a membrane of uniform material, identical spring stiffness coefficients for all edges in the mesh lead to noticeable distortions.

Volino and Magnenat-Thalmann have also recognized that making all spring coefficients the same gives bad results, and give several heuristic formulas, based on "inverse mass" of vertices and other parameters, for computing spring coefficients [VMT97]. With the parameter settings they suggest, their formula differs from the one derived here. Possibly, some other assumption about inverse masses would bring theirs into agreement. However, it should be emphasized that their objective was to simulate many properties of cloth and textiles, rather than an ideal elastic membrane.

# 2 Isotropic Elastic Materials

For an isotropic, linearly elastic material, the relationship between stress and strain depends on two parameters of elasticity, called Young's modulus ($E$) and the Poisson coefficient ($\nu$) [TG51]. These parameters may vary by position in the material, but if they do not we say the material is *uniform*. For a membrane of constant thickness $t$, we write $E_2 = Et$, so that $E_2$ is the "two-dimensional Young's modulus". Similarly for a one-dimensional spring (also called truss), of constant cross-sectional area $a$, we write $E_1 = Ea$.

Recall that *stress* is the force per unit length due to deformation of the material, while *strain* is deformation per unit length, with deformation being the local change in length in a particular direction. Rigid body motions consisting of translations and rotations do not contribute to deformation.

Young's modulus is also called the *modulus of stiffness*, because it measures the material's resistance to deformation. The Poisson coefficient $\nu$ measures the tendency of the material to *shrink* in directions orthogonal to a stretching stress, or *expand* in directions orthogonal to a compression stress. All natural materials have $\nu \geq 0$. The assumption of incompressibility implies $\nu = 0.50$. Timoshenko and Goodier recommend using $\nu = 0.25$ for "most materials" [TG51].

# 3 Modeling Elastic Membranes

In elasticity terminology, a *membrane* is an idealized two-dimensional elastic material for which forces needed to bend the surface are negligible in comparison to those needed to stretch or compress it. The simplest case is a planar membrane. In most cases the finite element method approximates a nonplanar membrane by a collection of planar patches, although higher order surfaces are sometimes used [Whi85, Fen86]. We shall restrict attention to the case of planar triangular patches. To make the paper accessible to a wider audience, and to provide geometrical insights, we shall avoid the use of tensor notation in the development.

### Stresses and Strains

Consider first a planar surface with a given discretization in the form of a set of vertices

$$V = \{v_i,\, i = 1, \ldots, n\}\,,$$

a triangulated planar graph connecting those vertices, producing a set of non-overlapping triangles,

$$\{T_e,\, e = 1, \ldots, m\}\,.$$

We make no assumption about the regularity of the triangulation. We assume the locations of the vertices in $E^2$ (Euclidean 2-space) are given for the situation in which there are no stresses. This is called the *rest position*.

In any orthonormal coordinate system $(u, v)$, denoting stress components by $\sigma_{uu}$, $\sigma_{vv}$, and $\sigma_{uv}$, and denoting strain components by $\varepsilon_{uu}$, $\varepsilon_{vv}$, and $\varepsilon_{uv}$, we have

$$\varepsilon_{uu} = (\sigma_{uu} - \nu\sigma_{vv})/E_2 \tag{3}$$

$$\varepsilon_{vv} = (-\nu\sigma_{uu} + \sigma_{vv})/E_2 \tag{4}$$

$$\tfrac{1}{2}\varepsilon_{uv} = (1+\nu)\sigma_{uv}/E_2 \tag{5}$$

where $E_2$ and $\nu$ were defined in Section 2. We avoid a matrix notation for the relationship of $\sigma$ and $\varepsilon$, although it is seen in some engineering texts [BR75, Fen86], because the three components of $\sigma$ and of $\varepsilon$ are more appropriately viewed as $2 \times 2$ symmetric matrices, rather than 3-vectors.

### Change of Coordinates, Principal Directions

Suppose coordinate frame $(u, v)$ is rotated counter-clockwise from the coordinate frame $(x, y)$ by angle $\theta$. Let $R(\theta)$ denote the rotation matrix:

$$R(\theta) = \begin{bmatrix} \cos\theta & -\sin\theta \\ \sin\theta & \cos\theta \end{bmatrix} \tag{6}$$

so that $\binom{u}{v} = R(\theta)\binom{x}{y}$. Then stress matrices in different coordinate frames are related through the similarity transformation:

$$\begin{bmatrix} \sigma_{uu} & \sigma_{uv} \\ \sigma_{uv} & \sigma_{vv} \end{bmatrix} = R^{-1}(\theta) \begin{bmatrix} \sigma_{xx} & \sigma_{xy} \\ \sigma_{xy} & \sigma_{yy} \end{bmatrix} R(\theta) \tag{7}$$

For symmetric matrices, as is well known, there are two choices of $\theta$ that diagonalize the left-hand side, and are 90 degrees apart. These are called the principal directions for the stress. Similar remarks apply to the strain matrix, but note the factor of $\frac{1}{2}$ on the off-diagonal elements:

$$\begin{bmatrix} \varepsilon_{uu} & \frac{1}{2}\varepsilon_{uv} \\ \frac{1}{2}\varepsilon_{uv} & \varepsilon_{vv} \end{bmatrix} = R^{-1}(\theta) \begin{bmatrix} \varepsilon_{xx} & \frac{1}{2}\varepsilon_{xy} \\ \frac{1}{2}\varepsilon_{xy} & \varepsilon_{yy} \end{bmatrix} R(\theta) \tag{8}$$

### The Equilibrium Problem

Given a set of external forces acting along the edges of a discretized membrane, the equilibrium problem is to find a deformation that induces strains and stresses that balance the external forces. For an equilibrium solution to exist, the external forces and torques must sum to zero.

In the triangulated finite element formulation, the deformations at vertices, $\delta_j, j = 1, \ldots, n$, are related to the external forces loaded on those vertices, $f_i, i = 1, \ldots, n$, through a *stiffness matrix* $\mathbf{K}$ with elements $K_{ij}$. However, the elements $K_{ij}$ are not scalars. Since $\delta_j$ and $f_i$ are 2-vectors, $K_{ij}$ is best thought of as a *linear transformation* from $E^2$ to $E^2$. The interpretation of the linear transformation $K_{ij}$ is: $K_{ij}\delta_j$ is the elastic force experienced at vertex $i$ due to a displacement $\delta_j$ of vertex $j$. This interpretation is independent of the coordinate frame. If a coordinate frame is chosen, then of course $K_{ij}$ can be *represented by* a $2 \times 2$ matrix in that frame.

For the mesh to be in equilibrium, letting $\delta$ and $f$ be the vectors of $\delta_j$ and $f_i$, we have

$$\mathbf{K}\delta + f = 0 \tag{9}$$

The form of $K_{ij}$ depends on the finite element model being used.

## 4 Exact Simulation by Springs is Impossible

This section demonstrates the difficulties encountered in an attempt to simulate a linearly elastic material accurately by a spring mesh, using the same triangulated surface for both models. The problems are shown to arise even in the simplest case: a two-dimensional planar membrane of constant thickness, with the simplest membrane model (constant strain), and with uniform elasticity in the membrane.

### Constant Strain Model

The finite element model most often seen for membranes is commonly called the *constant strain* model [BR75, Whi85, Fen86, ZT89]. Each triangle's stress and strain functions are assumed to be constant over the triangle's surface. This ensures that each triangle deforms into a triangle, and the global deformation is a piecewise continuous function of position. Each triangle edge has a uniform force per unit length, which is the sum of an internal forces due to the stress and "body force" in the triangle, and external forces applied to that edge. "Body force" is usually weight. In equilibrium, the internal and external force at the edge sum to zero. The $\mathbf{K}$ matrix is computed by computing the contribution of each triangle separately, and summing.

Let the triangle $T_e$ have vertices $p$, $q$, and $r$ in counter-clockwise order. Fix a coordinate frame $(x, y)$ for definiteness. We use the notations $(x_p, y_p)$ for the position of $p$ and $(x_{qp}, y_{qp})$ as an abbreviation for $(x_q - x_p, y_q - y_p)$. Then $\mathbf{K}_e^{\mathrm{M}}$ is a $3 \times 3$ matrix, whose elements are representable in the $(x, y)$ frame as $2 \times 2$ matrices. The superscript "M" stands for "membrane" (as opposed to spring mesh).

$$\mathbf{K}_e^{\mathrm{M}} = \begin{bmatrix} K_{pp}^{\mathrm{M}} & K_{pq}^{\mathrm{M}} & K_{pr}^{\mathrm{M}} \\ K_{qp}^{\mathrm{M}} & K_{qq}^{\mathrm{M}} & K_{qr}^{\mathrm{M}} \\ K_{rp}^{\mathrm{M}} & K_{rq}^{\mathrm{M}} & K_{rr}^{\mathrm{M}} \end{bmatrix} \tag{10}$$

where

$$K_{pp}^{\mathrm{M}} = \frac{E_2}{4\mathrm{area}(T_e)(1-\nu^2)} \begin{bmatrix} y_{rq}^2 + \left(\frac{1-\nu}{2}\right) x_{rq}^2 & -\left(\frac{1+\nu}{2}\right) y_{rq} x_{rq} \\ -\left(\frac{1+\nu}{2}\right) y_{rq} x_{rq} & x_{rq}^2 + \left(\frac{1-\nu}{2}\right) y_{rq}^2 \end{bmatrix} \tag{11}$$

$$K_{pq}^{\mathrm{M}} = \frac{E_2}{4\mathrm{area}(T_e)(1-\nu^2)} \begin{bmatrix} y_{rq} y_{pr} + \left(\frac{1-\nu}{2}\right) x_{rq} x_{pr} & -\nu y_{rq} x_{pr} - \left(\frac{1-\nu}{2}\right) y_{pr} x_{rq} \\ -\nu x_{rq} y_{pr} - \left(\frac{1-\nu}{2}\right) x_{pr} y_{rq} & x_{rq} x_{pr} + \left(\frac{1-\nu}{2}\right) y_{rq} y_{pr} \end{bmatrix} \tag{12}$$

and other components are found by cyclic permutation of $(p, q, r)$. In the above equations, $E_2$ is the two-dimensional Young's modulus, and $\nu$ is the Poisson coefficient, both being properties of the material.

### Spring Meshes

Now let us consider a different elasticity problem, analysis of an arrangement of pin-jointed trusses. This problem is equivalent to what is usually called a "spring mesh" in computer graphics literature. That is, each elastic element is one-dimensional, elements are "pinned" together at the vertices, so they may rotate freely. Stretching or compressing an element from its "rest length" produces a one-dimensional stress. We shall begin with a planar arrangement, with linear elasticity. This is one of the earliest problems to be analyzed with the finite element method [TCMT56].

Let us consider the same triangle as above: edges $(p, q)$, $(q, r)$, and $(r, p)$, in their rest positions. In addition, we specify the rest lengths and spring stiffness coefficients as $L_{qp}$, $k_{qp}$, etc. We continue to abbreviate $(x_q - x_p)$ as $x_{qp}$, etc. The stiffness matrix for the triangle of springs (or trusses), $\mathbf{K}_e^{spring}$, is again a $3 \times 3$ matrix whose elements are represented in the $(x, y)$ frame as $2 \times 2$ matrices. The superscript "S" stands for "spring mesh". We have [BR75, ZT89]:

$$K_{pp}^{\mathrm{S}} = E_1 \begin{bmatrix} \frac{k_{qp} x_{qp}^2}{L_{qp}^3} + \frac{k_{pr} x_{pr}^2}{L_{pr}^3} & \frac{k_{qp} x_{qp} y_{qp}}{L_{qp}^3} + \frac{k_{pr} x_{pr} y_{pr}}{L_{pr}^3} \\ \frac{k_{qp} x_{qp} y_{qp}}{L_{qp}^3} + \frac{k_{pr} x_{pr} y_{pr}}{L_{pr}^3} & \frac{k_{qp} y_{qp}^2}{L_{qp}^3} + \frac{k_{pr} y_{pr}^2}{L_{pr}^3} \end{bmatrix} \tag{13}$$

$$K_{pq}^{\mathrm{S}} = E_1 \begin{bmatrix} -\frac{k_{qp} x_{qp}^2}{L_{qp}^3} & -\frac{k_{qp} x_{qp} y_{qp}}{L_{qp}^3} \\ -\frac{k_{qp} x_{qp} y_{qp}}{L_{qp}^3} & -\frac{k_{qp} y_{qp}^2}{L_{qp}^3} \end{bmatrix} \tag{14}$$

and other components are found by cyclic permutation of $(p, q, r)$.

### Attempts to Equate Models

Now, if we want the spring triangle to simulate the constant-strain triangle, the obvious approach is to try to choose the stiffness coefficients of the three edges, $k_{qp}$, $k_{rq}$, $k_{pr}$, and the constant $E_1$ to bring the stiffness matrices of the two models into agreement. However, consider the constraint to make the upper-right matrix elements equal:

$$(K_{pq}^{\mathrm{S}})_{12} = (K_{pq}^{\mathrm{M}})_{12}.$$

By inspection we see that, in general, no such choice is possible. In particular, if $x_{qp}$ or $y_{qp}$ is zero, $k_{pq}$ cannot be solved for.

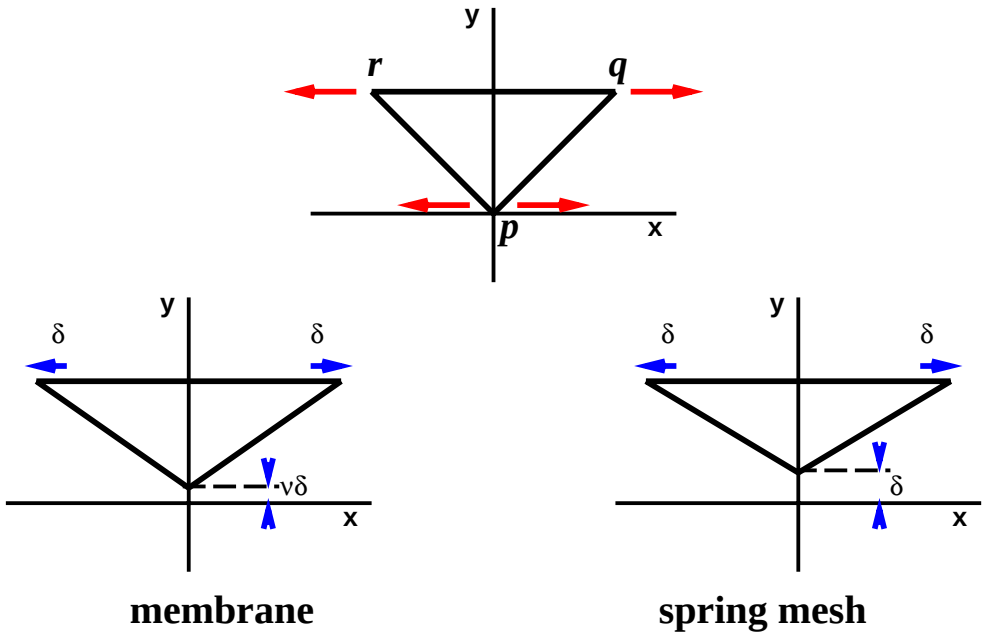


Figure 2: Isosceles right triangle subjected to horizontal forces (above). The two opposing forces at $p$ cancel. The triangle deforms differently under the membrane model (left) and the spring-mesh model (right). See Section 4 for discussion.

**Example 4.1** *For an isosceles right triangle with* $p = (0,0)$, $q = (1,0)$ *and* $r = (0,1)$, *the constraint* $K^{\mathrm{S}}_{pq,12} = K^{\mathrm{M}}_{pq,12}$ *is not satisfied by any choice of spring stiffness coefficients, because* $K^{\mathrm{S}}_{pq,12} = 0$, *while* $K^{\mathrm{M}}_{pq,12}$ *is negative.* □

Examination of the stiffness matrices associated with the constant strain model and the spring-mesh model has shown that, in general, no assignments of individual stiffness coefficients enable the stiffness matrix of the latter to agree with that of the former. However, there is a possible saving clause. The stiffness matrices actually are singular, and therefore do not uniquely determine a solution of the constraints. To see that stiffness matrices are singular, note that all rows sum to the $2 \times 2$ zero matrix. (Remember that the matrix elements are themselves $2 \times 2$ matrices.) Thus all stiffness matrices (of the kinds described, but the phenomenon is actually very general) have a zero eigenvalue. Therefore, one might hope that systems with differing stiffness matrices may have the same equilibria. However, we now show directly that the spring-mesh model cannot exactly simulate the membrane model, in sense of having the same equilibria. This applies for any physically realistic value of the Poisson coefficient, and variations of the example can make the point for physically unrealistic values, as well.

**Example 4.2** *Consider again an isosceles right triangle, only this time, for convenience, with* $p = (0,0)$, $q = (1,1)$ *and* $r = (-1,1)$. *Considering this as a membrane, assume a uniform, tensile, boundary stress of magnitude* $\sqrt{2}$ *is applied horizontally on edges* $(p,q)$ *and* $(r,p)$, *as shown in Figure 2. This is equivalent (in standard finite-element methodology) to horizontal tensile forces of magnitude 1 being applied at vertices* $q$ *and* $r$ *in the spring-mesh model. The two opposing forces at* $p$ *cancel.*

*For the membrane model, the internal stress at equilibrium is* $\sigma_{xx} = 2$, $\sigma_{yy} = 0$, *and* $\sigma_{xy} = 0$. *Therefore, the strain is* $\varepsilon_{xx} = 2/E_2$, $\varepsilon_{yy} = -2\nu/E_2$, *and* $\varepsilon_{xy} = 0$. *In other words, if edge* $(q,r)$ *increases in length by some small amount,* $2\varepsilon_{xx}$, *then the height (in* $y$*) decreases by* $\nu\varepsilon_{xx}$.

*However, for the spring-mesh model, since there is no net external force on* $p$, *the edges* $(p,q)$ *and* $(r,p)$ *are under no tension at equilibrium, and do not change length, despite the horizontal forces at* $q$ *and* $r$. *Since* $\sin(\pi/4) = \cos(\pi/4)$, *it follows that an increase in length of* $(q,r)$ *by any small amount,* $2\delta$, *is accompanied by a decrease in height of* $\delta$. *But* $\nu \leq \frac{1}{2}$ *for all physical materials. Therefore, no matter how the spring*

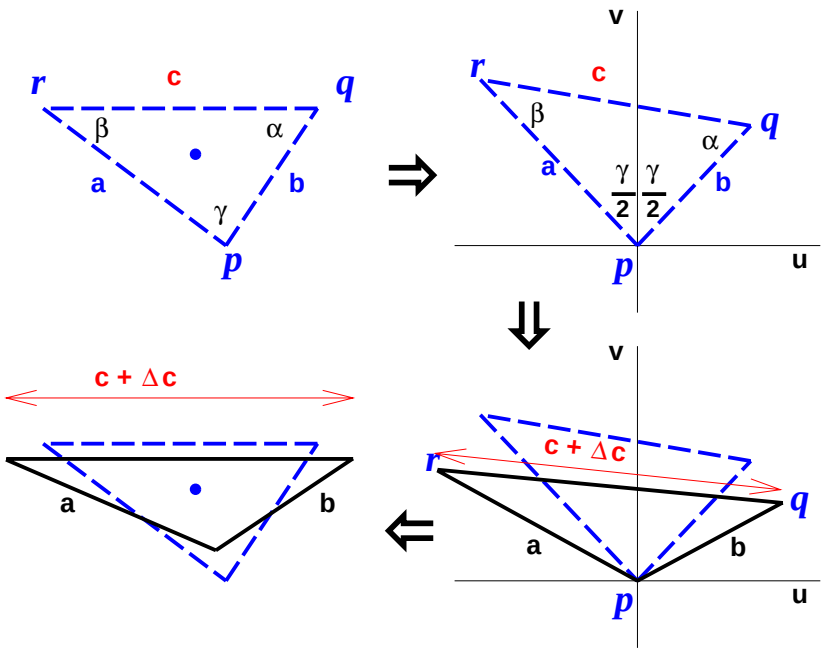


Figure 3: Undeformed triangular membrane (upper left, dashes), is rotated into a frame such that the $v$-axis bisects the angle $\gamma$ (upper right). A constant strain with $u$ and $v$ axes as principal directions deforms the triangle (lower right, solid-lined figure), which is then rotated back to make the upper edge horizontal (lower left, solid-lined figure). The second rotation is slightly different from the inverse of the first. The overall effect is the same as if the triangle were a spring mesh and a stretching force were applied horizontally at the ends of edge $c$. See Section 5 for discussion.

---

*stiffness for $(q, r)$ is chosen, the spring-mesh deformation cannot agree with the membrane deformation for horizontal external forces.* □

Given that an exact simulation is not possible for all stresses, it is natural to ask whether some natural class of stresses can be simulated exactly. It turns out that the class of *uniform* stresses can be simulated exactly, but the results are unlikely to be useful, so we shall omit the derivation. To cause a triangle of springs to behave like an elastic membrane under uniform stress, it is necessary to set the spring stiffness coefficients of each edge proportional to the cotangent of the opposite angle: $k_a \sim \cot\alpha$, etc., in Figure 3. However, this implies that the hypoteneuse of a right triangle has zero stiffness, and an edge opposite an obtuse angle has *negative* stiffness.

## 5 Constant Strain Approximation by Spring Meshes

Let us consider from first principles the problem of assigning spring stiffness coefficients to the edges of a triangle in such a way that the triangle will deform in the same manner as an isotropic elastic membrane, at least to the first order effects, as modeled by the constant strain model. That is, we limit consideration to the case that the external forces are uniformly distributed along each edge (different edges may have different forces – only the distribution is uniform). Also, we are concerned only with linear, equilibrium deformations. Therefore, we assume that the net external force and torque are zero.

Consider a triangle with edges $a$, $b$, and $c$ in counter-clockwise order, and edge $c$ horizontal, as shown in Figure 3, left. Let $\alpha$, $\beta$, and $\gamma$ be the opposing angles, as shown. Now suppose horizontal opposing external forces are applied at the ends of edge $c$, say a stretching force $\mathbf{f}$ at vertex $q$ and $-\mathbf{f}$ at vertex $r$, for definiteness.

First, suppose that the triangle consists of pin-connected springs (or trusses). Then, clearly edge $c$ will elongate, and edges $a$ and $b$ will not change length. Moreover, edge $c$ will remain horizontal. Assuming a

uniform distribution of mass, the center of gravity will not move, since no net work is done on the body. Therefore the solid-lined triangle in the lower left part of the figure represents the equilibrium position. Notice that the lower vertex elevates by exactly twice the amount that edge $c$ descends, to maintain the center of gravity. The amount of elongation of edge $c$ is defined as $\Delta|c|/|c|$, where "$|c|$" denotes the length of edge $c$, and "$\Delta|c|$" denotes the change in length. For a given $\mathbf{f}$, this elongation depends only on $|c|$ and $k_c$, the spring stiffness for edge $c$.

Now, suppose that the triangle consists of a membrane modeled by the constant strain model. The horizontal opposing external forces are distributed uniformly along edges $a$ and $b$ with force-per-unit-length of $-\mathbf{f}/a$ and $\mathbf{f}/b$. These boundary forces must be balanced by internal stress to achieve equilibrium.

The question is, for what family of internal stresses will the corresponding strains be such that the lengths of $a$ and $b$ do not change? This question has an elegant geometrical answer, which is indicated in the upper right panel of Figure 3. The key is to rotate into the coordinate frame $(u, v)$ such that the $v$-axis bisects the angle $\gamma$ (after that vertex is translated to the origin).

Now, *any* constant stress whose principal directions are the $u$ and $v$ axes will produce identical elongations in edges $a$ and $b$. (Recall that *elongations* are $\Delta|a|/|a|$ and $\Delta|b|/|b|$, not $\Delta|a|$ and $\Delta|b|$.) This follows from the observation that the slopes of edges $a$ and $b$ are equal in magnitude, although opposite in sign. For example, a positive stress $\sigma_{uu}$ increases the $u$-location of the rightmost vertex by $b\sin(\gamma/2)\sigma_{uu}/E_2$ and decreases the $u$-location of the leftmost vertex by $a\sin(\gamma/2)\sigma_{uu}/E_2$. This stress *decreases* the $v$-locations of the rightmost and leftmost vertices by $\nu b\cos(\gamma/2)\sigma_{uu}/E_2$ and $\nu a\cos(\gamma/2)\sigma_{uu}/E_2$, respectively. By similar triangles, the *relative* change in length, which is the strain, is the same for edges $a$ and $b$. Similar remarks apply to a stress $\sigma_{vv}$. For small elongations, the effects of $\sigma_{uu}$ and $\sigma_{vv}$ may be superposed.

Since any constant stress whose principal directions are the $u$ and $v$ axes will produce identical elongations in edges $a$ and $b$, it suffices to characterize the family of such stresses that produce *zero* elongation in edge $b$, leading to the lower right panel of Figure 3. For stresses in this family, we can find the relationship between $E_2$ and the resulting change of length $\Delta|c|$. This can be done in closed form, but seems to require some rather involved trigonometry, as described below. Those wishing to skip the technicalities may proceed to Eq. 24.

**Details of Strain Analysis**

For small elongations in the $u$ and $v$ directions, the elongation of edge $b$ is zero just when vertex $q$ is displaced in a direction orthogonal to edge $b$ (see lower right panel of Figure 3); i.e.,

$$\frac{\Delta v}{\Delta u} = \frac{-\sin(\gamma/2)}{\cos(\gamma/2)} \tag{15}$$

The family of stresses that satisfies this condition is given by

$$\frac{\cos(\gamma/2)(-\nu\sigma_{uu}+\sigma_{vv})}{\sin(\gamma/2)(\sigma_{uu}-\nu\sigma_{vv})} = \frac{-\sin(\gamma/2)}{\cos(\gamma/2)} \tag{16}$$

which can be rewritten as

$$\sigma_{vv}((1+\nu)\cos\gamma+(1-\nu)) = \sigma_{uu}((1+\nu)\cos\gamma-(1-\nu)) \tag{17}$$

Letting $(\Delta u, \Delta v)$ denote the displacement of vertex $q$, and letting $\Delta|c|$ denote the change in the *length* of edge $c$, for small elongations (ignoring second order terms), by choice of the $(u, v)$ frame, and Eq. 16, we have

$$\Delta|c| = \frac{4|a|\Delta u\,\sin(\gamma/2)}{|c|} = \frac{2\sin(\alpha)\Delta u}{\cos(\gamma/2)} \tag{18}$$

where the relation $(|a|/|c|) = (\sin\alpha/\sin\gamma)$ and half-angle identities were used. But

$$\Delta u = \left(\frac{|b|\sin(\gamma/2)}{E_2}\right)(\sigma_{uu}-\nu\sigma_{vv}) \tag{19}$$

Now, let $f$ denote the magnitude of the force stretching edge $c$ (with $f < 0$ to denote a compression force). Recall that in the spring mesh model, $k_c$, the spring stiffness coefficient of edge $c$, is related to $f$ through the equation:

$$f = k_c \Delta |c| \tag{20}$$

Now, switching to the constant strain membrane model, we obtain an equation for $f$ in terms of this model's elasticity parameters, so that equating the two expressions for $f$ we obtain a relationship among the spring-mesh parameter $k_c$, the membrane parameter $E_2$, and the geometry of the triangle.

Define $\theta = (\alpha - \beta)/2$. This is the direction parallel to edge $c$, relative to the $u$-axis. Then the stress in direction $\theta$, denoted as $\sigma_\theta$, is given by Eq. 7

$$\sigma_\theta \;=\; \cos^2\theta \sigma_{uu} + \sin^2\theta \sigma_{vv} \tag{21}$$

Next, $\sigma_{vv}$ can be eliminated from the above equation by use of Eq. 17, giving:

$$\sigma_\theta \;=\; \left( \frac{(1+\nu)\cos\gamma + (1-\nu)(\cos(\alpha-\beta))}{(1+\nu)\cos\gamma + (1-\nu)} \right) \sigma_{uu} \tag{22}$$

To conform to the constant strain model, it is necessary to assume additional opposing forces of size $f$ at the vertex $p$ (as in Figure 2, top), so that the stress along edges $a$ and $b$ is constant. Thus the total force exerted on side $a$ is $2f$, and similarly for side $b$. This gives the boundary condition [TG51]

$$\sigma_\theta \;=\; \frac{2f}{|a|\sin\beta} = \frac{2f}{|b|\sin\alpha} \tag{23}$$

**Geometrically-Based Stiffness Coefficient**

Combining Eqs. 17–23, we obtain

$$\Delta|c| \;=\; \frac{f}{k_c} \;=\; \frac{4|b|\sin\alpha\sin(\gamma/2)}{E_2\cos(\gamma/2)} \left(1 - \nu\frac{\sigma_{vv}}{\sigma_{uu}}\right)\sigma_{uu} \tag{24}$$

$$\frac{1}{k_c} \;=\; \frac{4\sin(\gamma/2)}{E_2\cos(\gamma/2)} \left( \frac{(1-\nu^2)(1+\cos\gamma)}{(1+\nu)\cos\gamma + (1-\nu)\cos(\alpha-\beta)} \right) \tag{25}$$

To solve for $k_c$, recall that $\alpha + \beta + \gamma = \pi$, and use half-angle identities:

$$k_c \;=\; \frac{E_2}{(1-\nu^2)} \left( \frac{\sin\alpha\sin\beta - \nu\cos\alpha\cos\beta}{2\sin\gamma} \right) \tag{26}$$

Finally, using the sine law and relationships among area, edge length and angles:

$$k_c \;=\; \left(\frac{E_2}{1+\nu}\right) \frac{\text{area}(T_e)}{|c|^2} + \left(\frac{E_2\,\nu}{1-\nu^2}\right) \frac{(|a|^2 + |b|^2 - |c|^2)}{8\,\text{area}(T_e)} \tag{27}$$

This formula can be evaluated just using the rest lengths of $a$, $b$, and $c$, with the aid of the relationship:

$$\text{area}(T_e) \;=\; \tfrac{1}{4}\sqrt{(|a|+|b|+|c|)(|a|+|b|-|c|)(|a|-|b|+|c|)(-|a|+|b|+|c|)} \tag{28}$$

Corresponding formulas may be obtained for $k_a$ and $k_b$ by the obvious renaming.

The coefficient derived, $k_c$, applies for *one* triangle of which $c$ is an edge, but unless $c$ is a boundary edge, $c$ occurs in *two* triangles, so the two individual coefficients are added (because forces due to stress in each triangle add) to give the total stiffness coefficient for edge $c$ in the overall spring mesh.

For an obtuse triangle, and $\nu > 0$, Eq. 27 should be treated with care. Since $(|a|^2 + |b|^2 - |c|^2) < 0$ in this case, when $c$ is the long edge, the value of $k_c$ could be negative. It is doubtful if this is physically justifiable.

To avoid such problems, our experiments always use $\nu = 0$, giving a simpler form, in which stiffness varies as area over length squared:

$$k_c = \frac{E_2 \,\mathrm{area}(T_e)}{|c|^2} \qquad \text{when } \nu = 0 \tag{29}$$

However, if the method of creating the mesh guarantees not to create obtuse triangles, the more complex form may give a closer approximation. In our applications, no observable difference in quality was detected between $\nu = 0$ and $\nu = 0.25$. However, this may not hold for other applications, and users are encouraged to experiment and draw their own conclusions.

### 5.1 Extension to Three Dimensions

The formula Eq. 29 may be derived heuristically as follows. Let $h$ be the altitude from side $c$ to vertex $p$ (see Figure 3), and assume a stretching force $f$ horizontally at the ends of side $c$. Also assume opposing horizontal forces of $f$ at the vertex $p$ (as in Figure 2, top). Then $2f$ is distributed over vertical distance $h$, and the membrane can be decomposed into numerous horizontal strips of width $\Delta h$ that all respond to force increments $2f\Delta h/h$ independently. Each strip elongates by $\varepsilon = 2f/hE_2$. The strip adjacent to side $c$ stretches by an amount $\Delta c = 2fc/hE_2 = f/k_c$. Therefore, $k_c = hE_2/2c$. But $\frac{1}{2}hc = \mathrm{area}(T_e)$, so $k_c = E_2\,\mathrm{area}(T_e)/|c|^2$. Since $k_c$ has the same dimensions (force/length) as $E_2$, the scaling of triangles does not affect their stiffness coefficients, only their shape matters. We shall see that this property does not carry over to tetrahedra.

This idea can be extended to three dimensions by imagining a tetrahedron $T_e$ to be decomposed into numerous tubes parallel to one of its edges, $c$. We assume vertices $q$ and $r$ are connected by edge $c$, while vertices $p$ and $s$ complete the tetrahedron. Then a force parallel to edge $c$ acts on each tube independently, to produce an elongation of $\varepsilon = 3f/AE$, where $E$ is the 3D Young's modulus of the elastic material to be simulated, and $A$ is now the projected area of the tetrahedron in a direction orthogonal to edge $c$. (We are still assuming $\nu = 0$.) The coefficient 3 occurs because $f$ is propagated in opposing force pairs to *two* additional vertices ($p$ and $s$) to achieve a constant stress over the faces *q-p-s* and *r-p-s*. This is the three-dimensional analog of the top of Figure 2. But $\frac{1}{3}Ac = \mathrm{vol}(T_e)$, the volume of the tetrahedron, so we obtain the approximation

$$k_c = \frac{E\,\mathrm{vol}(T_e)}{|c|^2} \tag{30}$$

It is important to note that $k_c$ does *not* have the same dimensions as $E$. Consequently, the scale of a tetrahedron, not just its shape, affects the computed values of the spring stiffness coefficients. As before, the total stiffness coefficient for edge $c$ is obtained by summing the $k_c$ values calculated for each tetrahedron of which $c$ is an edge.

## 6 Experimental Results

The method described has been implemented for some test meshes, where the correct behavior is known from the construction, and well as some more realistic examples. For reasons discussed earlier, we used $\nu = 0$, as in Eq. 29, throughout the tests. This amounts to the rule that stiffness varies as area over edge length squared. Experimental results are illustrated in Figs. 4, 5, and 6.

In the first test a simple, hexagonal planar membrane was simulated. As shown in Figure 4, the discretization was irregular. The external forces were equal radial forces, applied at the six boundary vertices. Assuming a uniformly elastic membrane, the deformation should also be uniform, at least with the constant-strain membrane model. When all edges are assigned the same spring stiffness, noticeable distortion occurs at equilibrium. This distortion exists for smaller deformations as well; it is not merely a manifestation of nonlinearity. Another plausible idea is to assign the same one-dimensional Young's modulus ($E_1$) to all edges. Since $E_1$ is defined by $f = E_1\Delta c/c$, this heuristic implies that stiffness is inversely proportional to edge length. The same figure shows that comparable distortion occurs. However, when edges are assigned coefficients in accordance with Eq. 29, the distortion disappears.

In the second test, an isosurface was extracted, based on a potential field from two nearby spheres, forming a "skin" around the pair. The isosurface is represented as a triangulated mesh. Each triangle has a circle textured upon it, in its undeformed shape (some triangles did not get an entire circle). The widely varying sizes of the circles indicate the widely varying sizes of triangles in the isosurface. Because of the popularity of isosurfaces as a means of surface creation, we believe this test is indicative of effects that can be expected in practice. To induce a deformation, one sphere was pulled away from the other, with the "skin" constrained to stretch so that it surrounded them both. Then the skin was allowed to reach equilibrium, based on the spring mesh model. Now, for a uniformly elastic membrane the skin should deform fairly uniformly. At least, the deformations of nearby triangles should be approximately the same. The deformed circles become ellipses that demonstrate the effective strain in each triangle. Again, we see that setting all spring coefficients equal leads to widely varying strains. However, the use of Eq. 29 to assign coefficients produced significantly more uniform strains in the individual triangles.

This method has also been incorporated into an animal modeling program [WVG97a, WVG97b], in which the skin is modeled as a triangulated mesh with uniform $E_2$ and $\nu = 0$. Figure 6 shows the hind quarter of a "tiger" in a sequence of positions. In each position, the skin has been relaxed into approximate elastic equilibrium over the muscles and other underlying tissue.

# 7 Conclusion

We have derived an approximate formula for defining spring stiffness coefficients for each edge in terms of the geometry of the mesh triangles containing that edge. The resulting spring mesh approximates an isotropic elastic membrane, at least for small deformations. Experimental results presented indicate that the agreement is quite good for fairly large deformations as well. We have shown that an exact simulation is impossible.

Some questions deserve further study. Can a triangulation with many obtuse angles be transformed into one with few or no obtuse angles and produce better approximations? Can redundant springs overcome some defects in the approximation based on a single triangle mesh? Experimentation with three-dimensional problems is also important.

# Acknowledgments

This research was funded in part by Research and Development Laboratories, and by NSF Grant CDA-9115268. We thank Jane Wilhelms for use of test models and animal models for the experiments reported, and for help on reviewing background material. We thank the anonymous referees for valuable comments on improving the paper.

# References

[BR75] William H. Bowes and Leslie T. Russel. *Stress Analysis by the Finite Element Method for Practicing Engineers*. D. C. Heath, Lexington, 1975.

[BW98] David Baraff and Andrew Witkin. Large steps in cloth simulation. *Computer Graphics (ACM SIGGRAPH Proceedings)*, pages 43–54, July 1998.

[CG91] G. Celniker and G. Gossard. Deformable curve and surface finite elements for free-form shape design. *Computer Graphics (ACM SIGGRAPH Proceedings)*, 25:257–266, July, 1991.

[CZ92] David T. Chen and David Zeltzer. Pump it up: Computer animation based model of muscle using the finite element method. *Computer Graphics (ACM SIGGRAPH Proceedings)*, 26(2):89–98, July 1992.

[EDC96] Jeffrey W. Eischen, Shigan Deng, and Timothy G. Clapp. Finite-element modeling and control of flexible fabric parts. *IEEE Computer Graphics and Applications*, 16(5):71–80, September 1996.

[Fen86] R. T. Fenner. *Engineering Elasticity : Application of Numerical and Analytical Techniques.* Ellis Horwood Series in Mechanical Engineering. John Wiley, New York, 1986.

[FVdPT97] P. Faloutsos, M. Van de Panne, and D. Terzopoulos. Dynamic free-form deformations for animation synthesis. *IEEE Transactions on Visualization and Computer Graphics*, 3(3):201–214, 1997.

[KGC+96] R. M. Koch, M. H. Gross, F. R. Carls, D. F. von Buerin, G. Fankhauser, and Y. I. H. Parish. Simulating facial surgery using finite element models. *Computer Graphics (ACM SIGGRAPH Proceedings)*, pages 421–428, August 1996.

[LTW95] Yuencheng Lee, Demetri Terzopoulos, and Keith Waters. Realistic modeling for facial animation. *Computer Graphics (ACM SIGGRAPH Proceedings)*, pages 55–62, August 1995.

[Mil88] Gavin Miller. From wire-frames to furry animals. In *Graphics Interface '88*, pages 138–145, Edmonton, Alberta, June 1988.

[NG96] Hing N. Ng and Richard L. Grimsdale. Computer graphics techniques for modeling cloth. *IEEE Computer Graphics and Applications*, 16(5):28–41, September 1996.

[TCMT56] M. J. Turner, R. W. Clough, H. C. Martin, and L. C. Topp. Stiffness and deflection analysis of complex structures. *J. Aeronautical Science*, 23(9), September 1956.

[TF88] Demetri Terzopoulos and Kurt Fleischer. Modeling inelastic deformation: Viscoelasticity, plasticity, fracture. *SIGGRAPH '88 Conference Proceedings*, 22(4):269–278, August, 1988.

[TG51] S. Timoshenko and J. N. Goodier. *Theory of Elasticity.* McGraw-Hill Book Company, Inc., New York, second edition edition, 1951.

[TPBF87] Demetri Terzopoulos, John Platt, Alan H. Barr, and Kurt Fleischer. Elastically deformable models. *SIGGRAPH '87 Conference Proceedings*, 21(4):214, July 1987.

[TTG95] Demetri Terzopoulos, Xiaoyuan Tu, and Radek Grzeszczuk. Artificial fishes: Autonomous locomotion, perception, behavior, and learning in a simulated world. *Artificial Life*, 1:327–351, 1995.

[TW88] Demetri Terzopoulos and Andrew Witkin. Physically based models with rigid and deformable components. *IEEE Computer Graphics and Applications*, 8(6):41–51, November 1988.

[TW90] D. Terzopoulos and K. Waters. Physically-based facial modelling, analysis, and animation. *The Journal of Visualization and Computer Animation*, 1(2):73–80, 1990.

[TW91] Demetri Terzopoulos and Keith Waters. Techniques for realistic facial modeling and animation. In Nadia Magnenat-Thalmann and Daniel Thalmann, editors, *Computer Animation '91*, pages 58–74. Springer-Verlag, Geneva, 1991.

[VCMT95] Pascal Volino, Martin Courchesne, and Nadia Magnenat-Thalmann. Versatile and efficient techniques for simulating cloth and other deformable objects. *Computer Graphics (ACM SIGGRAPH Proceedings)*, pages 137–144, August 1995.

[VMT97] Pascal Volino and Nadia Magnenat-Thalmann. Developing simulation techniques for an interactive clothing system. In *Proceedings Int'l Conf. on Virtual Systems and MultiMedia*, pages 109–118, Geneva, Switzerland, 1997. IEEE Comput. Soc.

[Whi85] R. E. White. *An Introduction to the Finite Element Method with Applications to Nonlinear Problems.* John Wiley, New York, 1985.

[WVG97a] Jane Wilhelms and Allen Van Gelder. Anatomically based modeling. In *Computer Graphics (ACM SIGGRAPH Proceedings)*, Aug. 1997.

[WVG97b] Jane Wilhelms and Allen Van Gelder. Anatomically Based Modeling. Technical Report UCSC-CRL-97-10, CS Dept., University of California, 225 A.S., Santa Cruz, CA 95064, April 1997.

[ZT89] O. C. Zienkiewicz and R. L. Taylor. *The Finite Element Method*, volume 1. McCraw-Hill Book Company, fourth edition, 1989.

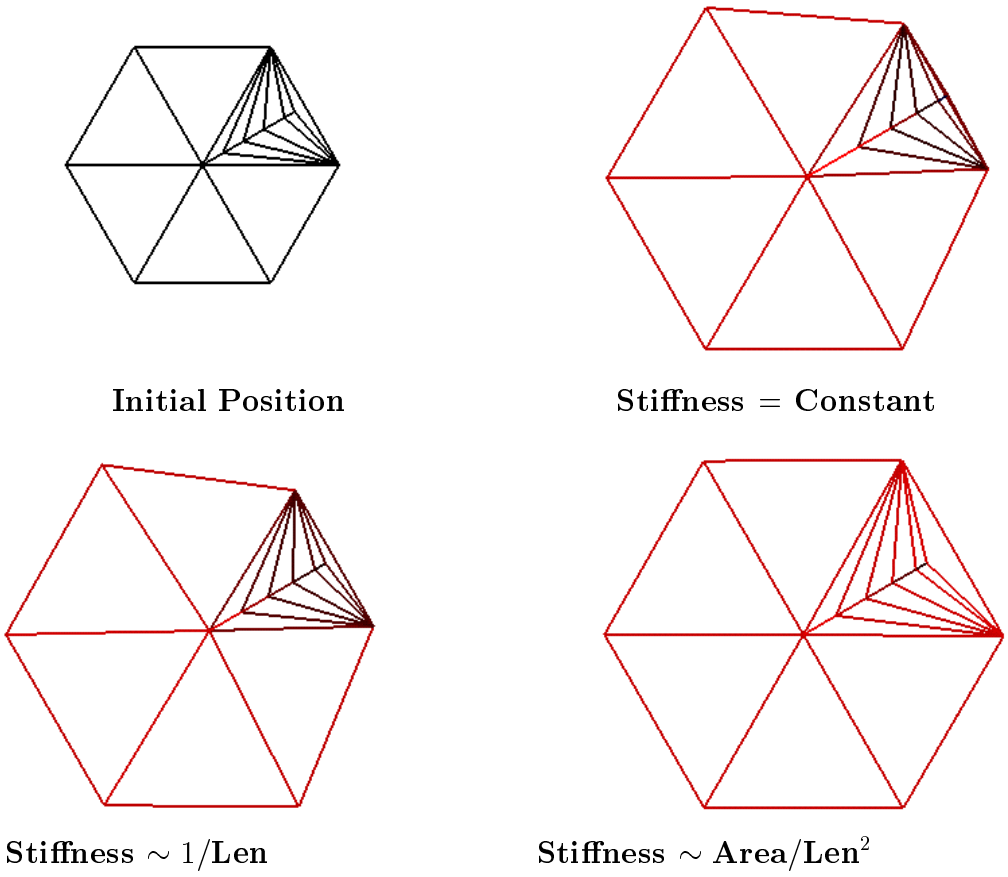


Figure 4: Comparison of effect of spring stiffness coefficients on test membrane, assumed to be of a homogeneous material, as discussed in Section 6. The irregularly subdivided hexagonal membrane at upper left is subjected to a constant outward radial force at the six boundary vertices. Correct behavior is a uniform expansion. Remaining pictures show various simulations by spring meshes: constant stiffness (upper right), constant one-dimensional Young's modulus, which implies stiffness inversely proportional to edge length (lower left), and stiffness proportional to area over length squared, as derived in the text (lower right).

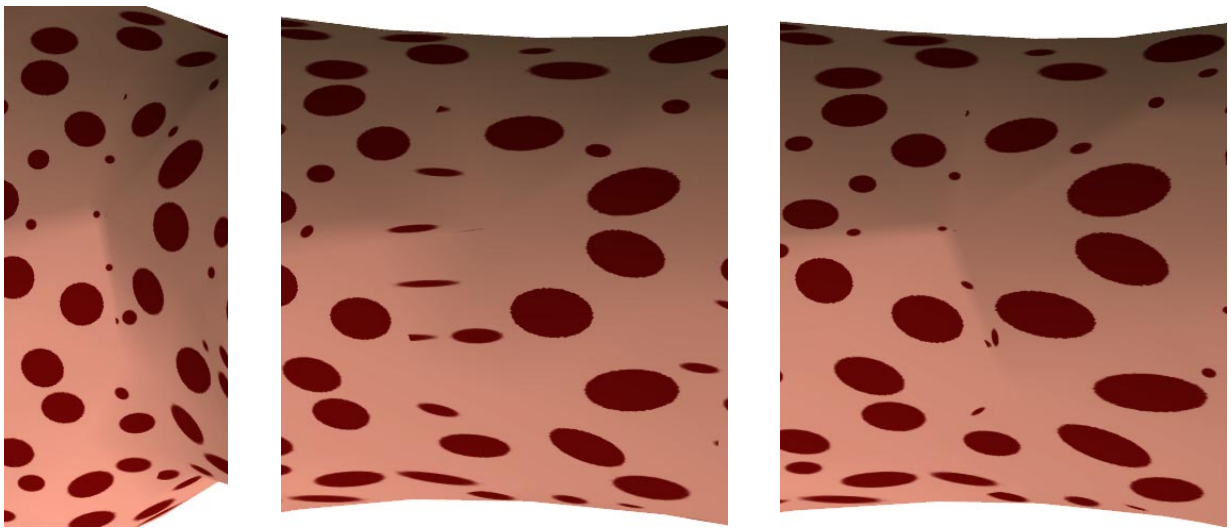

Figure 5: The choice of spring stiffness coefficients affects a stretched elastic membrane. In the initial triangulated mesh, each triangle contains a circle. Because the mesh is quite irregular, the size of the triangles (and circles) varies. The rest configuration is shown at left. The stretched configuration at equilibrium is shown center and right, in two versions. Use of a constant stiffness coefficient for all edges is shown at center; notice many of the small circles are distorted irregularly. At the right, values based on Eq. 27 are used for stiffness coefficients, and the circles are distorted more regularly.

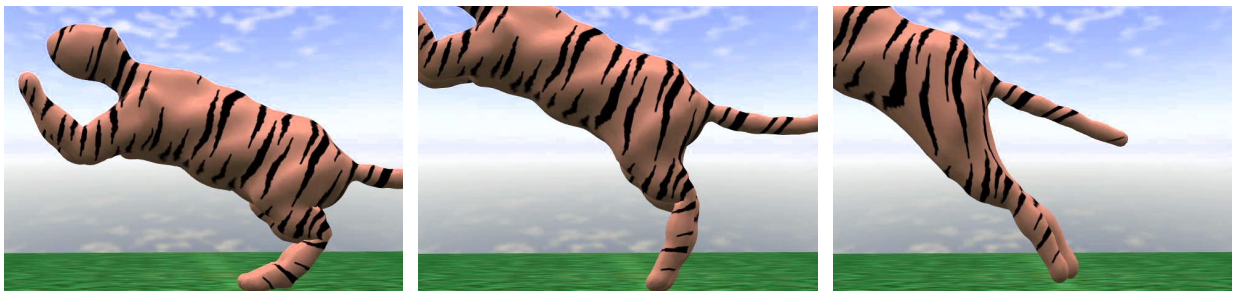

Figure 6: An application of an elastic triangulated mesh. The "tiger" skin is modeled as a spring mesh with stiffness coefficients calculated as described in the paper. As the underlying skeleton moves, the muscles deform, and the skin should move smoothly with the nearby muscle to create a realistic motion.